

Here

$$\Delta E_1 = E(p\frac{1}{2}) - E(p\frac{3}{2}) + \text{pairing},$$

$$\Delta E_2 = E(d\frac{3}{2}) - E(d\frac{5}{2}) + \text{pairing},$$

where p is the number of the odd nucleons in the shell (odd-hole nucleons in the case $J = \frac{3}{2}^+$), n_1 is the number of odd nucleons in the adjacent shell $J = \frac{5}{2}$, and $E(l, j)$ is the single-particle excitation energy. The numerical values are calculated using the parameters given in Ref. 7.

We remark that in the first five cases, the corrections (if not zero) decrease the Schmidt value (V_s is negative); in the last case, the correction is positive as expected. The experimental trend is very well reproduced; corrections to these relations are small and do not spoil the agreement with our previous analysis.

In concluding, our results suggest the following:

- (i) Also in the light nuclei neutrons and protons can be treated independently, at least as far as $\sum_i^A \sigma_{i3} \tau_{i3}$ and $\sum_i^A \sigma_{i3}$ operators are concerned.
- (ii) The effect of the antisymmetrization of neutrons and protons on the shell is not so important as believed, also in the light nuclei.⁶
- (iii) A simple configuration mixing calculation using an extreme $j-j$ coupling scheme as unperturbed basis gives quantitative agreement between experiment and theory and explains satisfactorily the linear quenching.
- (iv) In our approximation ($V_s - V_t = 0$) the configuration mixing does not affect the SU(4)

symmetry (the state $S = \frac{1}{2}$, $T = \frac{1}{2}$ is not mixed to higher S, T states).

Thus the quenching mechanism in the LS coupling scheme is due to the presence of a mixing between different L : for example, for $J = \frac{3}{2}$ states, between $L = 1$ and $L = 2$. This puts in evidence that the magnetic moments lie between the Schmidt lines.

¹R. Leonardi and M. Rosa-Clot, Phys. Rev. Letters **21**, 377 (1968).

²R. Leonardi, *Cargèse Lectures in Physics*, (Gordon and Breach, New York, 1969), Vol. III.

³R. Leonardi and M. Rosa-Clot, Columbia University Report No. NYO-1932-144 (to be published), and Lettere Nuovo Cimento **1**, 829 (1969).

⁴In a recent paper, K. Sugimoto [Phys. Rev. **182**, 1051 (1969)], who performs considerations similar to those suggested in Refs. 2 and 3, explicitly points out the similarity between $\Sigma(A)$ and $\Sigma T(A)$.

⁵This formula improves the assumption $\mu_0 = \text{const}$ of Refs. 1-3. In a different form this relation is $[\mu_p(A) - J] / \mu_n(A) = -1.20$. This is an enlargement of the De-Shalit relation $(g_s - g_l)_p / (g_s - g_l)_n = -1.20$.

⁶J. P. Elliott and A. M. Lane, *Handbuch der Physik*, edited by S. Flügge (Springer-Verlag, Berlin, 1959), Vol. 39, p. 294.

⁷H. Noya, A. Arima, and H. Horie, Progr. Theoret. Phys. Suppl. **8**, 33 (1959).

⁸R. J. Blin-Stoyle and M. A. Perks, Proc. Phys. Soc. (London) **A67**, 885 (1954).

⁹We consider only the mixing between different j with the same l . (See Ref. 8).

SYNCHROTRON EMISSION AT STRONG RADIATIVE DAMPING*

C. S. Shen

Department of Physics, Purdue University, Lafayette, Indiana 47907

(Received 22 December 1969)

The motion and radiation of a relativistic classical charged particle in an intense magnetic field is analyzed when the radiative reaction force is comparable with the Lorentz force. Their significance for cosmic problems, especially the acceleration and radiation of cosmic-ray electrons in pulsars, is discussed.

In the conventional theory of synchrotron radiation the electron is treated as a classical particle whose trajectory is unaffected by radiation energy losses. In an intense magnetic field two corrections, the quantum-mechanical nature of the particle and the effect of radiation reaction on the particle's trajectory, should be considered. The quantum effect becomes important when the energy of emitted photons is comparable with the particle energy, i.e., when $\hbar\gamma^2\omega_H/\gamma mc^2 = \gamma\omega_H/\alpha\omega_0 \rightarrow 1$,¹ where $\gamma = E/mc^2$ represents

the energy of particle and $\omega_H = eH/mc$ characterizes the strength of the field; $\omega_0 = 3mc^3/2e^2 = 1.8 \times 10^{23} \text{ sec}^{-1}$ is the fundamental frequency of a free electron and $\alpha = e^2/\hbar c$ is the fine structure constant. The radiative-reaction effect becomes important when the reaction force becomes comparable with the Lorentz force, or equivalently, when the lifetime of an electron against synchrotron radiation becomes comparable with its Larmor period, i.e., when $\gamma^2\omega_H/\omega_0 \approx 1$.¹

Quantum-mechanical treatment of synchrotron

radiation has been studied in the past.^{2,3} Recently Chiu and Canuto⁴ have considered its application to pulsar emissions. On the other hand, synchrotron radiation at strong radiative damping has never been exploited in detail.⁵ Comparison of the two parameters, $\gamma\omega_H/\alpha\omega_0$ and $\gamma^2\omega_H/\omega_0$, shows that radiative reactions predominate quantum effects in an intense magnetic field for particles of energy $\gamma > 137$. Therefore, for highly relativistic particles one can always study the effect of strong radiative damping within the realm of classical electrodynamics. In present-day laboratory experiments, the effect of radiative reaction on synchrotron emission is always negligible. But this may not be true for cosmic problems, especially when the radiation is emitted by high-energy electrons in a strong magnetic field, such as the magnetosphere of a neutron star. Take the Crab pulsar as an example; the copious x- and gamma-ray emissions from the

surrounding nebula require a continuous supply of high-energy electrons up to $E \sim 10^5$ BeV.⁶ Several authors⁷ have suggested the magnetosphere, or its near surroundings, of the central neutron star to be the site of acceleration. Take $H = 10^8$ G to be a typical field strength in regions of acceleration and emission. We observe that for electrons of energy between 50 and 10^7 BeV the condition $1 \leq \gamma^2\omega_H/\omega_0 \leq \alpha\gamma$ prevails. This condition implies a strong coupling between field and particle but with negligible interference from the quantum effect.

In this paper, we shall first analyze the trajectory of a classical relativistic particle with strong radiative damping, then proceed to compute the frequency spectrum of its radiation. Implications of the present work in astrophysics will be discussed briefly along the way.

The general equation of motion of a classical charged particle in an electromagnetic field is¹

$$\dot{U}_i = \frac{e}{mc} F_{ik} U^k + \omega_0^{-1} (\ddot{U}_i - \frac{1}{c^2} U_i \dot{U}^k \dot{U}_k), \quad i = 1 \text{ to } 4, \quad (1)$$

where F_{ik} is the electromagnetic field tensor, U_i is the four-velocity, $\dot{U}_i = dU_i/d\tau$, and $d\tau$ is the proper time.

The first term on the right of Eq. (1) represents the Lorentz forces which ordinarily control the particle motion. The second and third terms represent forces due to radiation reaction. The ratio of these two forces, as mentioned above, is given by $R = f_R/f_L = \gamma^2\omega_H/\omega_0$, which also represents the fractional energy loss per revolution. The validity of Eq. (1) has been discussed extensively in the literature.^{1,8} Of all restrictions the most stringent one is that classical electrodynamics breaks down at $\gamma\omega_H/\omega_0 \sim 1/137$ due to the quantum effect. Hence Eq. (1) may be considered reliable at $R/\gamma \ll 1/137$. This restriction obviously does not exclude its application to cases of strong radiative damping ($R \geq 1$) for highly relativistic particles. We shall therefore solve Eq. (1) for finite values of R but neglect all higher order terms of γ^{-1} and $\gamma^{-1}R$.

The term $\dot{U}^k \dot{U}_k$ in Eq. (1) is a four-scalar; thus it must equal $\dot{U}^k \dot{U}_k$ in the instantaneous rest frame of the particle. In this particular reference frame the particle sees an electric field $\gamma\beta H \sin\Phi$, where Φ is the angle between the instantaneous velocity \vec{v} and the field \vec{H} . We find, to the lowest significant order of γ^{-1} and $\gamma^{-1}R$,

$$\dot{U}^k \dot{U}_k = \gamma^2 c^2 \omega_H^2 \sin^2\Phi [(1 + \dot{\gamma}/\omega_0\gamma)^2 - (\gamma\omega_H \sin\Phi/\omega_0)^2]. \quad (2)$$

With the help of Eq. (2), Eq. (1) can be solved to give $U_i(\tau)$. For practical purpose we must translate these covariant quantities to the ordinary space and time variables of the observer. Using the relation

$$t = \int_0^\tau \gamma(\tau') d\tau' = \frac{1}{c} \int_0^\tau U_4(\tau') d\tau',$$

we find after some tedious calculations

$$\frac{d\gamma}{dt} = -\frac{\gamma^2 \omega_H^2 \sin^2\Phi}{\omega_0} \left[1 - 6 \left(\frac{R}{\gamma} \right)^2 \sin^2\Phi \right], \quad (3)$$

$$\gamma(t) = \gamma_0 \left[1 + R_0 (\omega_H t / \gamma_0) (1 - 6 R_0^2 \gamma_0^{-2} \sin^2\Phi_0) \sin^2\Phi_0 \right]^{-1}, \quad (4)$$

$$v_1(t) = v_0[1-h(t)] \sin\Phi_0 \cos f(t), \tag{5.1}$$

$$v_2(t) = v_0[1-h(t)] \sin\Phi_0 \sin f(t), \tag{5.2}$$

$$v_3(t) = v_0 \cos\Phi_0, \tag{5.3}$$

where

$$f(t) = \left(1 + \frac{R_0 \sin^2\Phi_0 \omega_H t}{2\gamma_0}\right) \frac{\omega_H t}{\gamma_0}.$$

The subscript 0 denotes initial values at $t=0$. We have chose $\vec{H} \parallel z$ axis and $v_2(0) = 0$. The leading term in $h(t)$ is $\sim (R_0^2/\gamma_0^2)(\omega_H t/\gamma_0)$, which is entirely negligible unless $t \sim \gamma_0^3/R_0^2\omega_H$, but the particle is then nonrelativistic and the approximation we used is no longer valid. The term $h(t)$ is kept in Eq. (5) just to indicate the smallness of the variation in the particle pitch angle.

The trajectory of the particle as described by Eq. (5) is a shrinking helix (Fig. 1). The radius of curvature $\rho(t) = v^2/v_\perp$ decreases as $(1 + \gamma_0^{-1} \times R\omega_H t \sin^2\Phi)^{-1}$; after completing the first cycle both ρ and the particle energy are reduced by a factor of $(1 + 4\pi R \sin\Phi)^{-1/2}$. Two interesting points may be brought to attention: (1) The radiative reactions modify the instantaneous energy loss rate only slightly [to the order of $(R/\gamma)^2$]. This results from the fact that forces exerted by radiative damping are mostly along the direction of \vec{v} while the force exerted by the magnetic field is perpendicular to the velocity. For comparable parallel and perpendicular forces the total radiation due to the parallel component is of the order $1/\gamma^2$ smaller than that from the perpendicular component. Thus within the range of validity of classical electrodynamics radiative reaction

forces cannot change the instantaneous emission rate significantly, although alteration of the orbit of the particle could be large, hence the effect on the frequency distribution of the total radiation may be significant. (2) The decay rate of the angle between the velocity vector \vec{v} and the field \vec{H} is much slower (by a factor of γ^{-2}) than the decay rate of the particle energy. In the nonrelativistic case radiation draws all of its energy from the perpendicular component of motion. Therefore, the particle's pitch angle decreases with the reduction of its energy.⁵ A nonrelativistic particle injected randomly into the field would lose about $\frac{2}{3}$ of its initial energy, then stream along the field line with no further radiation energy losses. But this is not true for a relativistic particle. Although the particle's radius of gyration decreases quickly at strong radiative damping, the pitch angle remains practically constant. In the pulsar theory of origin of cosmic rays, radiation energy losses have in general been neglected. One of the arguments is that synchrotron radiation only drains the transverse momentum of particles. Therefore in a regular field, such as the neutron-star magnetosphere, a particle will stream out along the field lines and retain a substantial portion of its energy in the longitudinal component. This, as has been shown, is not true. For example, in a region of $H = 10^6$ G, the energy of a 100-BeV electron reduces to 100 MeV after traveling a distance 1 km (and gyration of about 40 cycles). Unless an electric field of enormous strength⁹ exists to prevent the curving of particle trajectories, relativistic electrons can hardly get out of the vicinity of the magnetosphere, not to mention accelerations.

The radiation spectrum of a particle is related to its trajectory by¹⁰

$$\frac{dI(\omega)}{d\Omega} = \frac{e^2\omega^2}{4\pi^2c^2} \left| \int_{-\infty}^{\infty} \vec{n} \times (\vec{n} \times \vec{v}) e^{i\omega(t - \vec{n} \cdot \vec{r}/c)} dt \right|^2. \tag{6}$$

It is well known that radiation emitted by a relativistic particle is concentrated in the forward direction of motion. Inspection of Eq. (5) shows that the velocity vector \vec{v} repeats its direction after certain time intervals. Thus a distant observer located on the surface of the velocity cone will record successive pulses of radiation at those moments when the particle is moving toward him. However, unlike the case of ordinary synchrotron emission, the orbit of the particle at strong radiative damping is not periodic. The time intervals between successive

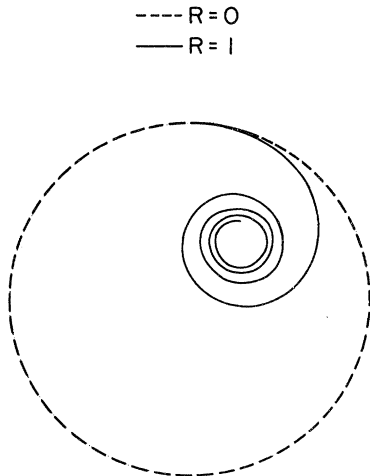


FIG. 1. Orbit of a charged particle moving in the plane perpendicular to \vec{H} at $R = \gamma^2\omega_H/\omega_0 = 1$.

pulses, as well as the character of each pulse are not the same. For simplicity, let us assume the particle is moving in the plane perpendicular to \vec{H} . Since radiation damping does not change the pitch angle of the particle, results obtained in this special case can be extended to the general case following the same procedure used in conventional synchrotron theory.¹¹ We shall indicate the modifications introduced due to $v_3 \neq 0$ in the final paragraph. But here let us consider an observer located near the x axis with the particle moving in the x - y plane. From Eq. (5) we see that he receives bursts of radiation when $v_2(t) = 0$, or at

$$t = t_n = \left[\frac{(1 + 4\pi n R_0)^{1/2} - 1}{R_0} \right] \frac{\gamma_0}{\omega_H}$$

while the energy of the emitting particle is $\gamma(t_n) = \gamma_n = \gamma_0(1 + 4\pi n R_0)^{-1/2}$. The observer records a series of closely packed pulses. The time interval between successive pulses decreases while the duration of each pulse increases. The total radiation from the particle is the superposition

of all pulses. Mathematically, this is equivalent to writing the integral in Eq. (6) as a summation, i.e.,

$$\int_{-\infty}^{\infty} dt \rightarrow \sum_{n=0}^N \int_{(t_{n-1} + t_n)/2}^{(t_n + t_{n+1})/2} dt.$$

(Assume the particle injected into emission region just before $t = 0$.) The n th term in the summation represents the Fourier transformation of the amplitude of the n th pulse. Since the radiation of each pulse is concentrated within a time interval $(\gamma_n^2 \omega_H)^{-1}$ around t_n where the duration between successive pulses is $\gamma_n \omega_H^{-1}$, the limits of integration for each term in the summation can be replaced by $\pm\infty$ after a suitable transformation of variables. With this approximation, Eq. (6) can be evaluated, following the usual procedure of computing the radiation spectrum from an ultrarelativistic particle,

$$\frac{dI(\omega)}{d\Omega} = \frac{e^2 \omega^2}{3\pi^2 c \gamma_0^2 \omega_H^2} [A_{\parallel}^2(\omega) + A_{\perp}^2(\omega)]. \quad (7.1)$$

$A_{\parallel}^2(\omega)$ and $A_{\perp}^2(\omega)$ correspond to the two polarization components,

$$A_{\parallel}^2(\omega) = \sum_{n=0}^N a_n^2(\theta) b_n^{-1} \left[K_{2/3}^2\left(\frac{\omega}{\omega_n}\right) + \left(\frac{R_0}{\gamma_0}\right)^2 a_n^{-1}(\theta) K_{1/3}^2\left(\frac{\omega}{\omega_n}\right) \right], \quad (7.2)$$

$$A_{\perp}^2(\omega) = \sum_{n=0}^N a_n(\theta) b_n^{-1} \gamma_0^2 \theta^2 K_{1/3}^2\left(\frac{\omega}{\omega_n}\right), \quad (7.3)$$

where

$$a_n(\theta) = 1 + \gamma_0^2 \theta^2 + 4\pi n R_0, \quad b_n = 1 + 4\pi n R_0, \quad \omega_n = 3\gamma_0^2 \omega_H b_n^{1/2} [a_n(\theta) - R_0^2 / \gamma_0^2]^{-3/2},$$

and θ is the colatitude angle the observer made with the orbiting plane. $K_{2/3}$ and $K_{1/3}$ are modified Bessel functions. In Eq. (7) the difference between the spectrum of individual pulse and the classical expression for radiation emitted by a relativistic particle of energy γ_n and radius of curvature ρ_n is of the order of $(R_n / \gamma_n)^2$, a result consistent with Eq. (3).

All information about the radiation is contained in Eq. (7). Of particular interest for astrophysical applications are the polarization and frequency distribution of radiation. The frequency distribution of the total energy emitted by a particle of initial energy γ_0 is

$$I(\gamma_0, \omega) = \int \frac{dI(\omega)}{d\Omega} d\Omega = \frac{2e^2 \omega}{\sqrt{3} c \gamma_0 \omega_H} \sum_{n=0}^N b_n \int_{2b_n^2 \omega / 3 \gamma_0^2 \omega_H}^{\infty} K_{5/3}(x) dx + O\left(\frac{R_0}{\gamma_0}\right)^2. \quad (8)$$

$I(\gamma_0, \omega)$ is plotted in Fig. 2 for $R = 8 \times 10^{-3}$, 1 and 10. In the high-frequency range $\xi = \omega / \gamma_0^2 \omega_H > (1 + 4\pi R_0)^{-1}$ the spectrum varies as $\xi^{1/2} e^{-2\xi/3}$. For $\xi < (1 + 4\pi R_0)^{-1}$ the spectrum varies as $\xi^{-1/2}$. If we follow Eq. (6) strictly, the upper limit N of the summation in Eq. (8) should be ∞ , the $\xi^{-1/2}$ variation would extend to zero (or to $\omega = \omega_H$ where the approximation used breaks down). However, summation to ∞ corresponds to observing the particle for an infinite period of time. For

a finite observation period T , emission from the latter pulses (at low ω) will be cut off, then $I(\gamma_0, \omega)$ would have a maximum at $\xi_f = (1 + R_0 \omega_H T / \gamma_0)^{-2} = \gamma^2(T) / \gamma_0^2$. For $\xi < \xi_f$, $I(\omega)$ varies as $\xi^{1/3}$. It should be clear now that the conventional synchrotron radiation theory, for which the frequency spectrum varies as $\xi^{1/3}$ at $\xi < 1$, is applicable when the particle loses a negligible amount of energy within the observation time. In a strong

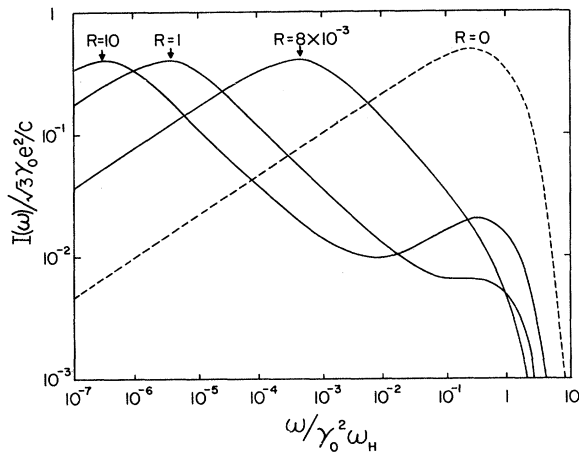


FIG. 2. Spectrum of synchrotron radiation with radiative reaction. $R = \gamma_0^2 \omega_H / \omega_0$ approximately represents the ratio between the reaction force and the Lorentz force. $I(\omega)$ (measured in units of $\sqrt{3} \gamma_0 e^2 / c$) is the energy radiated per unit frequency by a particle of initial energy $\gamma_0 m c^2$. The change of slope at very low frequency is due to finite observation.

magnetic field ξ_c is much less than 1. If $H = 10^6$ G, for example, $\xi_f \cong 1/\gamma_0^2$ (i.e., $\omega_f = \omega_H$) for $T = 10^{-3}$ sec. So in practice the frequency spectrum of radiation emitted by a relativistic electron from a region of $H = 10^6$ G can always be taken as $\xi^{-1/2}$ when $\xi < 1$. In order to compare the variation of $I(\omega)$ with respect to R we have nevertheless chosen $T = 10^{-5}$ sec in Fig. 2. It is interesting to note that even when $R = 8 \times 10^{-3}$, for which most of the radiation is in the frequency range below $R\omega_0 = 10^{21}$ sec $^{-1}$, the damping effects are already significant.

The polarization of the radiation is given by

$$\Pi(\omega) = \frac{A_{\parallel}^2(\omega) - A_{\perp}^2(\omega)}{A_{\parallel}^2(\omega) + A_{\perp}^2(\omega)}$$

The values of $\Pi(\omega)$ are plotted in Fig. 3 for the same sets of parameters as $I(\omega)$. In the frequency range of $(1 + 4\pi R_0)^{-1/2} \gg \xi_f$, $\Pi(\omega)$ has the common value of 0.695 for all values of R . At $\xi \ll \xi_f$, Π drops to 0.5.

The results obtained above are easily generalized to cover the case that the particle's longitudinal velocity $v_3 \neq 0$. One needs to replace H by $H \sin \Phi_0$ in all computations. In addition $I(\gamma_0, \omega)$ should be divided by $\sin^2 \Phi_0$ to take care of the Doppler effect on t_n , the interval between pulses.¹¹

In reality one of course observes radiation from an ensemble of electrons. If the particles are injected into the emission region in a narrow beam and all possess the same energy, as one

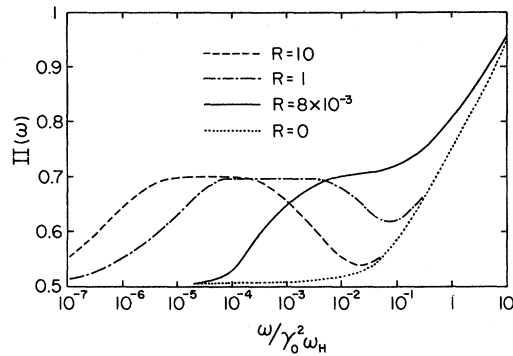


FIG. 3. Polarization of synchrotron radiation from a single particle.

would expect from a laboratory experiment, the power spectrum would look exactly like that shown in Fig. 2. For cosmic problems the distribution of the particle is usually near isotropic and covers a wide range of energy, and the fields which accelerate the particles are of course more complicated than the uniform magnetic field assumed in this paper. Therefore, application of the present work to actual astrophysical problems will be discussed elsewhere.¹² However, it is illustrative to consider here the simple case of a power-law electron distribution injected isotropically into the emission region, where the influence of the strong magnetic field dominates all other effects. The power emitted from the region per unit solid angle is

$$J(\omega) = (1/4\pi) \int Q(\gamma_i) \langle I(\omega, \gamma_i) \rangle d\gamma_i, \quad (9)$$

where

$$\langle I(\omega, \gamma_i) \rangle = (1/2\pi) \int_0^{2\pi} I(\omega, \gamma_i (1 + R_i \psi)^{-1/2}) d\psi$$

denotes average over the azimuth angle of the injection direction of the particles. $Q(\gamma_i)$ represents the injection rate.¹³ For the case of $Q(\gamma_i) = Q_0 \gamma_i^{-\alpha}$ up to a maximum γ_∞ , the radiation spectrum at $\omega < \gamma_\infty^2 \omega_H$ is

$$J(\omega) \sim \omega^{-1/2} \text{ for } \alpha < 3, \quad (10.1)$$

$$\sim \omega^{-(\alpha-2)/2} \text{ for } \alpha > 3. \quad (10.2)$$

This result, which is derived under the condition that the emitting particles lose most of their energy in a time shorter than the observation time, may be compared with the results obtained in the ordinary synchrotron radiation theory, in which the frequency spectrum is proportional to $\omega^{-(\alpha-1)/2}$ for all values of α .

I wish to thank C. H. Chan, T. K. Kuo, and J. Meyer for helpful discussions. A part of the work was carried out during the author's visit

to Goddard Institute for Space Studies at New York. I wish to thank Dr. Robert Jastrow for hospitality.

*Work supported by NASA Grant No. 4947-52-13969.

¹See for example, L. Landau and E. Lifshitz, Classical Theory of Fields (Addison-Wesley, Reading, Mass., 1951), Chap. 9.

²T. Erber, *Rev. Mod. Phys.* **38**, 626 (1966).

³N. P. Klepikov, *Zh. Eksperim. i Teor. Fiz.* **26**, 19 (1954).

⁴H. Y. Chiu and V. Canuto, *Phys. Rev. Letters* **22**, 415 (1969).

⁵G. N. Plass, *Rev. Mod. Phys.* **33**, 37 (1961). In this reference the relativistic equation of motion including radiative damping is solved for the limit case of energy loss per revolution very small.

⁶R. C. Haynes *et al.*, *Astrophys. J.* **151**, L9 (1968).

⁷T. Gold, *Nature* **218**, 731 (1968); J. F. Gunn and

J. P. Ostriker, *Phys. Rev. Letters* **22**, 728 (1969).

⁸P. A. M. Dirac, *Proc. Roy. Soc. (London)*, Ser. A **167**, 148 (1938); J. A. Wheeler and R. P. Feynman, *Rev. Mod. Phys.* **17**, 157 (1945).

⁹F. C. Michel, *Phys. Rev. Letters* **23**, 247 (1969); F. Occhionero and M. Demianski, *Phys. Rev. Letters* **23**, 1128 (1969).

¹⁰J. D. Jackson, Classical Electrodynamics (Wiley, New York, 1963), Chap. 14. All notations used in this paper for spectrum calculation follow this reference.

¹¹V. L. Ginzburg and S. I. Syrovatskii, *Ann. Rev. Astron. Astrophys.* **7**, 375 (1969).

¹²C. S. Shen, to be published.

¹³Since $I(\gamma_0, \omega)$ is the total energy radiated per unit frequency by an electron of initial energy γ_0 , and the emitting electrons lose a substantial fraction of their energy within a few revolutions, the power emission is logically given by integration over the injection (or production) spectrum of the particle instead of the equilibrium spectrum, which may not exist under the prescribed circumstances.

MEASUREMENT OF PRIMORDIAL HELIUM ABUNDANCE FROM THE STAR μ CASSIOPEIAE*

Dennis Hegyi† and David Currott‡

Palmer Physical Laboratory, Princeton University, Princeton, New Jersey 08540

(Received 6 October 1969)

A measurement of the separation between the components of the binary star μ -Cassiopeiae to yield the stellar masses has been made. Applying the mass-luminosity law, we find a helium abundance $Y \sim 0$ where a 1σ and 2σ random error allows, respectively, $Y \sim 0.05$ and $Y \sim 0.34$. The measured abundance places an upper limit on the helium production in a big bang cosmological model.

μ Cassiopeiae is an old binary star system whose chemical composition is thought to be characteristic of the early stages of formation of the galaxy. A determination of the primordial helium abundance¹ is of current interest to physicists as a potential means of distinguishing between relativity theories. Because μ Cas is too cool to excite the helium spectrum, the star's helium abundance cannot be determined spectroscopically. Alternatively, the mass-luminosity law of the theory of stellar interiors can be applied. This law relates the mass and luminosity of a star to its chemical composition, i.e., once the mass and luminosity of a star are known, the star's helium abundance can be determined if its metal abundance is known. In the case of μ Cas, the luminosity and metal abundance of the brighter component μ Cas A is known, but its mass is unknown. From kinematics it is possible to find the masses of stars that are members of a binary system. Because μ Cas is a binary, and enough orbital information is available, the mass of μ Cas A can be found with one measurement

of the angular separation between the stars.

The problem has been to resolve optically the two stars which are approximately 1 arc sec apart and which differ in intensity by a factor of 100 at $\lambda \sim 5000 \text{ \AA}$.² The resolution is limited by inhomogeneities in the earth's atmosphere which distort the incoming plane wave fronts to the extent that a good stellar image has a half-width 2 arc sec in diameter.

The present experiment is based on the assumption that light rays from closely separated stars travel along almost identical paths through the atmosphere; hence at each instant of time, images of the two stars, although they are moving about, always maintain the same separation. An image analyzer has been constructed which scans the stellar image in a few msec, quickly enough to freeze the image, thereby taking advantage of the constant instantaneous separation between the components. The stars are imaged on a rotating wheel with narrow slits so that the light transmitted through the wheel as a function of time is characteristic of the image profile.